Self-ratiometric fluorescence approach based on plant extract-assisted synthesized silver nanoparticles for the determination of vanillin

Mohamed A. El Hamd[1,2,a], Mahmoud El-Maghrabey[3,4,a]*, Saud Almawash[1], Rania El-Shaheny[4], Galal Magdy[5]

[1] Department of Pharmaceutical Sciences, College of Pharmacy, Shaqra University, Shaqra 11961, Saudi Arabia.

[2] Department of Pharmaceutical Analytical Chemistry, Faculty of Pharmacy, South Valley University, Qena 83523, Egypt.

[3] Graduate School of Biomedical Sciences, Course of Pharmaceutical Sciences, Nagasaki University, 1-14 Bunkyo-machi, Nagasaki 852-8521, Japan.

[4] Department of Pharmaceutical Analytical Chemistry, Faculty of Pharmacy, Mansoura University, Mansoura 35516, Egypt.

[5] Pharmaceutical Analytical Chemistry Department, Faculty of Pharmacy, Kafrelsheikh University, Kafrelsheikh P.O. Box 33511, Egypt.

[a] These authors have equal contributions to the manuscript.

***Correspondence:** Mahmoud El-Maghrabey: mh-elmaghrabey@nagasaki-u.ac.jp

Abstract

The current study designed and applied a novel self-ratiometric fluorescent nanosensor composed of green-synthesized silver nanoparticles (Ag-NPs) to determine vanillin in adult and infant foods and human plasma. A straightforward microwave-assisted approach was proposed for synthesizing Ag-NPs in less than 1 minute using a reducing agent, *Tailed Pepper* seed extract. The synthesized Ag-NPs had a strong fluorescence with an intense emission band at 360 nm and shoulder peak at 430 nm when excited at 265 nm. Upon interaction with vanillin, the fluorescence peak of Ag-NPs at 360 nm decreases in a concentration-dependent manner while being shifted to a longer wavelength, 385 nm. Meanwhile, the shoulder fluorescence peak at 430 nm is only slightly affected by vanillin addition. Thus, a new Ag-NP self-ratiometric probe was designed and validated for vanillin determination using the peak at 385 nm and the shoulder peak at 430 as two built-in reference peaks. The optimized system accurately measured vanillin with a detection limit of 9.0 ng/mL and linear range of 0.05 – 8.0 µg/mL without needing pre-derivatization or high-cost instrumentation. The method successfully measured vanillin in adult and infant milk formula, biscuits, and human plasma samples with high percent recoveries (95.3-104.6%) and excellent precision (RSD (≤ 3.85%).

Keywords: Silver nanoparticles; Ratiometric fluorescence probe; *Tailed Pepper*; Vanillin; Food and milk; Plasma

1. Introduction

Vanillin, 4-hydroxy-3-methoxybenzaldehyde, is a flavour additive added to many adult and infant foods and drinks. Chemically, vanillin possesses many functional groups, including aldehyde, ether, and phenol, which are the reason for its unique, pleasant odour. Exposure of a person to vanillin through foods, drinks, or household products contributes to the body's absorption of vanillin, which may cause toxicity to the liver and kidneys [1]. Therefore, the Food and Drug Administration (FDA) states that the concentration of vanillin in food should not exceed 70 mg/kg. In addition, vanillin-containing foods are forbidden from being used in the formula for 0–6 months-old infants due to the potential health problems induced by excess ingestion, including impaired liver, kidney, and spleen functions [2]. On the other hand, due to the expenses of natural sources, only a small percentage of natural-originated vanillin is used in beverages and foods, which represent only 0.2% of the market requirement [3]. As a result, most of the used vanillin in food and industry is artificially obtained via synthetic or biotechnological production. Therefore, a sensitive, rapid, and reliable method for the determination of vanillin in food samples is essential to confirm its allowed limits.

Vanillin has been detected in food samples using a variety of methods, including spectrophotometry [4], turn-off spectrofluorimetry [5–8], electrochemistry [9–12], capillary electrophoresis [13], chromatographic-mass spectrometric techniques [14, 15], and very recently chemiluminescence assay [16]. These reported methods, however, have a number of disadvantages, including the need for large volumes of organic solvents [14] and highly skilled workers [14, 15], lack of sensitivity [4], and great quantities of toxic solvents, [13–15], in addition to the time-consuming and expensive assembly of electro-chemosensors [9–12], as well as the use of hazardous hydrogen peroxide and expensive luminol reagents [16]. Additionally, none of these methods are extended to biological samples. Although the previously developed methods for measuring vanillin in different matrices offer acceptable sensitivity, selectivity, and sensitive extraction procedures, it is still necessary to assess vanillin at nano-concentration levels in food and/or biological samples.

The need to monitor dangerous additives or contaminants in adult and infant food samples, such as vanillin, has resulted in a growing demand for rapid and precise analyte information. Fluorescence-based sensing techniques are a straightforward, inexpensive, extremely sensitive, and selective analytical method [17]. Despite having successful applications for qualitative and quantitative fluorescence analysis of vanillin by fluorescence turn-off [5–8], these methods' sensitivity and accuracy are vulnerable to instrument signal instability and probe concentration,

which can result in false positives and poor selectivity. By detecting the relative fluorescence fluctuations at two different wavelengths of a fluorescent probe, ratiometric fluorescence probes or methodologies are suited to solve these issues, minimizing detection error [18]. As a result, the goal of the current study was to combine the ratiometric technique with the standard fluorescence-based detection to optimize the measurement strategy and improve its sensitivity.

Silver nanoparticles (Ag-NPs) are catching the attention of researchers owing to their numerous environmental, industrial, medical, and pharmaceutical applications. Top-down and bottom-up are the two main methods used to prepare nanomaterials. However, chemical agents used in preparing Ag-NPs have adverse effects on the environment and are potential toxicity risks. Thus, there is a current interest in the environmentally friendly synthesis of nanoparticles using extracts from various plant parts, bacteria, fungi, algae, or animal metabolites [19].

The current study aimed to establish a new sensitive and convenient platform for selective determination and confirmation of the acceptable limit of the presence of vanillin in adult foods and milk formula. Furthermore, a preclinical study was established to evaluate its level in human plasma samples. Plants have many constituents that exhibit potential as reducing agents, such as flavonoids, alkaloids, saponins, phenolics, and tannins [20]. Various plant species have been utilized in the synthesis of nanoparticles, including cinnamon, aloe vera, and many other plants [21]. Plants possess several advantageous characteristics that render them a superior choice for the synthesis of Ag-NPs compared to alternative approaches. These advantages include their reduced toxicity, enhanced safety, and widespread availability [22]. In the present study, we synthesized Ag-NPs using a plant extract, *tailed pepper* seed extract, in ultrashort time using a microwave for the first time. The synthesized Ag-NPs show a strong fluorescence at 360 nm and a shoulder fluorescence at 430 nm. Upon the interaction with vanillin, the fluorescence peak of ANPs at 360 nm decreases in a concentration-dependent manner while being shifted to a longer wavelength. Meanwhile, the shoulder fluorescence peak at 430 nm is only slightly affected by the addition of vanillin. Thus, we designed and validated a new Ag-NP self-ratiometric probe for vanillin determination using the peak at 385 nm and the shoulder peak at 430 as two built-in reference peaks. In this strategy, we free two birds with one key by developing a self-ratiometric fluorescence approach based on two built-in references using microwave/plant extract-assisted bio-synthesized silver nanoparticles without the need for complicated fabrication of multi-signal probe composites. The main challenge for the designed probe was using an excitation wavelength in the UV region ($\lambda_{excitation}$ = 265 nm), which

could make the probe prone to interferences by biomatter, but this issue was resolved by the self-ratiometric nature of the probe, which corrected any potential interference.

The proposed method has been tested for validity according to FDA and ICH guidelines [23]. Furthermore, the greenness and whiteness aspects of the ratiometric fluorescent nanosensor have been assessed. This was accomplished by employing four green metrics, namely the Greenness index represented by a spider diagram [24], the Analytical Greenness tool (AGREE) [25], the AGREEprep for evaluating sample preparation [26], and the Complex Green Analytical Procedure Index (ComplexGAPI) for assessing the pre-analysis steps [27]. Additionally, the whiteness score [28] was determined to indicate the level of sustainability of the developed nanosensor and was favourably compared with the previously reported method for vanillin determination.

2. Experimental

The used instruments, materials, reagents and standard solutions, together with the method of quantum yield measurement, are mentioned in detail in the supplementary file.

2.1.Synthesis of silver nanoparticles (Ag-NPs) using Tailed pepper extract and microwave

The experimental conditions employed for the synthesis were meticulously investigated, encompassing several factors such as the quantities of powdered tailed pepper, duration of extraction boiling, temperature of extraction heating, volume and concentration of $AgNO_3$, volume of *Tailed pepper* extract, and duration of microwave heating. Following multiple experimental iterations, the materials and method outlined subsequently yielded the most favourable fluorescence intensity and superior stability of the synthesized Ag-NPs. Consequently, these specific components and procedures were employed for the synthesis of the Ag-NPs. The optimum procedure was as follows:

One hundred mL of double-distilled water was used to boil 5.0 g of powdered tailed pepper for 10 min. After cooling, the resulting solution was filtered and centrifuged for 10 min at 10000 revolutions per minute, and the supernatant was stored in the refrigerator until needed. Next, 25.0 mL of $AgNO_3$ (1.0 mM) was mixed with 50.0 mL of *Tailed pepper* extract and was put in the microwave for 40 s. The obtained dark brown solution was kept in the refrigerator **(Fig. 1)**.

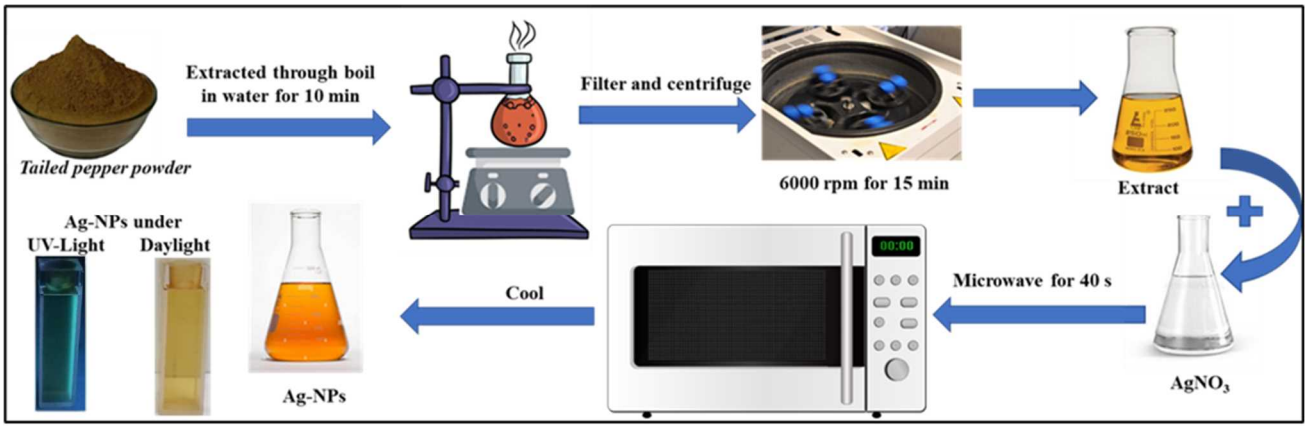

Fig. 1. Schematic presentation of the microwave/plant extract-assisted synthesis of Ag-NPs with an inset showing Ag-NPs under daylight and UV light. The tailed pepper powder was extracted by boiling it in water, then filtered, and then used as a reducing agent for AgNO3 employing microwave treatment.

2.2.Calibration plot

100.0 µL of Ag-NPs and 1.0 mL Britton-Robinson buffer were transferred into a group of 10-ml volumetric flasks. Different volumes of vanillin standard solution that yield a final concentration within the range of 0.05-8.0 µg/mL were added, and solutions were made up to 10 mL with distilled water and mixed well. The fluorescence intensity (FI) of Ag-NPs was determined at 360 nm after excitation at 265 nm at room temperature, and the shifted fluorescence peak at 385 nm and the shoulder fluorescence peak at 430 nm was used as dual built-in references. Two calibration plots were constructed using a fluorescence intensity ratio of (FI_{385}/FI_{360}) or (FI_{430}/FI_{360}) *versus* vanillin concentrations (µg/mL) then the regression equations were derived.

2.3. Preparation of real samples

Infant milk powder and biscuit samples were pretreated according to a reference method [29]. In short, the biscuit sample was powdered using a mortar and pestle. Then 0.5 g biscuit powder or milk powder was transferred separately into 15-mL centrifuge tubes and spiked with different concentrations of vanillin; then, the tubes were completed to 10 mL with ethanol. The mixture was sonicated for 1 h and then centrifuged at 5000 *rpm* for 10 min. Next, 1.0 mL of the supernatant was transferred to a 5-mL volumetric flask, followed by 1.0 mL Britton-Robinson buffer (pH 10) and 100.0 µL Ag-NPs. The flask contents were completed to the mark with distilled water to obtain the

final concentrations of vanillin (2.0, 4.0, 6.0, 8.0 µg/mL). The blank experiment was conducted similarly. Then, the spectrofluorimetric measurements were performed as mentioned in section "**2.2"**.

2.4.Procedure for human plasma

1.0 mL aliquots of human plasma were transferred to a series of 15-mL centrifugation tubes and spiked with increasing volumes of vanillin standard solution to obtain final concentrations of 2.0, 4.0, 6.0, and 8.0 µg/mL. The samples were diluted with ethanol to 5 mL and then mixed with a vortex for two minutes. The tubes were centrifuged at 10,000 rpm for 15 minutes. The supernatant from each tube was filtered through syringe filters (0.45 µm). The procedure described in section "2.5" was carried out in parallel with the blank experiment, and recovery was calculated.

3. Results and Discussion

A green approach has been optimized for the synthesis of Ag-NPs using a natural reductant, *Tailed pepper* seed extract. The *Tailed pepper* (*Piper cubeba*; Family *Piperaceae*) is a plant grown for its essential oil in Java and Sumatra (*Java pepper*). The *tailed pepper* contains a variety of antioxidant-active constituents, such as polyphenols, glycosides, tannins, and flavonoids that possess reducing activity [30]. *The tailed pepper* seed extract is preferred as a green-reducing agent due to its availability in many regions worldwide. It is cost-effective, safe, and non-toxic when compared to chemicals used in chemical reduction methods, such as sodium borohydride ($NaBH_4$) or N,N-dimethyl formamide. As with many other sensing techniques, using nanomaterials in ratiometric fluorescence probes has created intriguing sensing systems [19]. In this study, the synthesized Ag-NPs have been utilized for the construction of a highly sensitive self-ratiometric fluorescence probe for robust, reproducible, and accurate determination of vanillin in different food and milk products, as well as plasma samples. Compared to single-signal test, ratiometric sensing experiences results in less interference and can produce more precise results. By creating a self-ratiometric fluorescence technique based on two built-in references and using microwave/plant extract-assisted biosynthesis of Ag-NPs, we can free two birds with one key without the requirement for the time-consuming manufacture of multi-signal probe composites.

3.1. Characterization of silver nanoparticles (Ag-NPs)

The synthesized Ag-NPs showed strong blue-green fluorescence under UV light and dark orange colour under visible light (**Fig. 1 inset**). Their characterizations have been achieved through FT-IR spectrometry, HRTEM, UV-visible spectrophotometry, and spectrofluorimetry. The morphology and size of Ag-NPs were examined using HRTEM, which revealed that Ag-NPs were well separated with spherical shape and particle size ranged from 8 to 18 nm with average particle size of 11.0±2.1 nm **(Fig. 2A)**. In addition, FT-IR was used to study the surface functional groups of Ag-NPs **(Fig. 2B)**. The obtained spectrum showed different functional groups, including N-H (3448 cm^{-1}), C-H (2924 cm^{-1}), C=O (1705 cm^{-1}), C-C (1450 cm^{-1}), C-N (1200 cm^{-1}), and numerous out-of-plane C-H (600-800 cm^{-1}) as shown in **Fig. 2B**. This finding shows that self-functionalized hydroxyl, carbonyl, and amino groups on the surface of the synthesized Ag-NPs give the system excellent aqueous solubility and biocompatibility [31]. The UV-visible absorption spectra of $AgNO_3$ and Ag-NPs are shown in **Fig. 2C.** Ag-NPs displayed a maximum UV absorption peak at 390 nm. Two notable peaks indicated that their absorption shoulders were caused by the transition between the C=C and C=O bonds at the π–π^* and n–π^* positions, respectively [32].

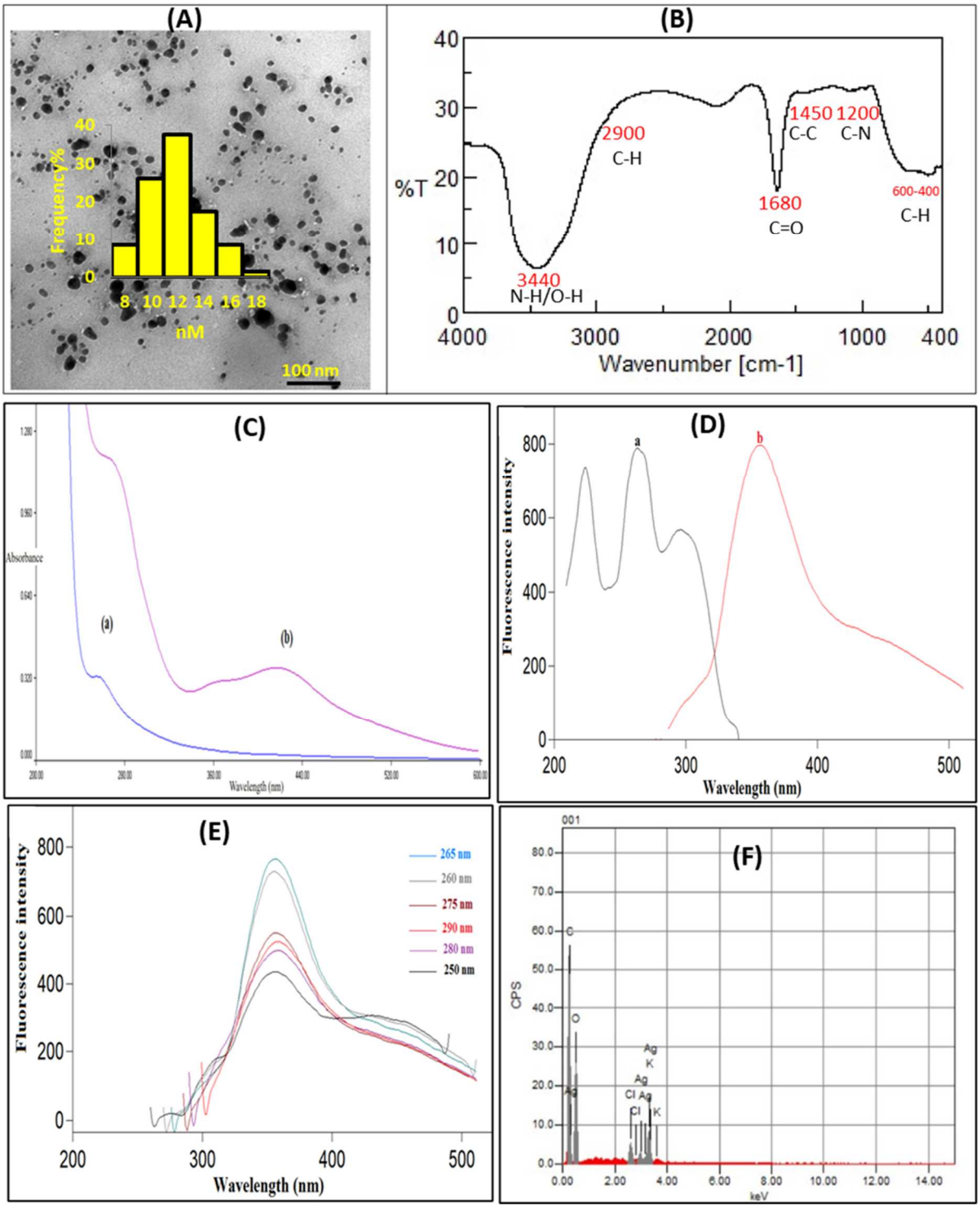

Fig. 2. The morphological and spectroscopic characterization of the synthesized AgNPs where (A) HRTEM images of Ag-NPs, (B) FT-IR spectrum of Ag-NPs elucidating its surface functional groups, (C) UV-visible absorption spectrum of (a) $AgNO_3$ and (b) Ag-NPs, (D) Ag-NPs fluorescence excitation and emission spectra (a, b), (E) the fluorescence emission spectra of the Ag-NPs at various excitation wavelengths (250–290 nm) showing excitation non-dependent emission, and (F) EDX spectrum of Ag-NPs.

Next, the fluorescence spectra of the synthesized Ag-NPs were studied, and it was found that it yielded maximum emission at 360 nm with shoulder fluorescence peak at 430 nm after excitation at

265 nm (**Fig. 2D**). Next, the quantum yield of Ag-NPs was also evaluated as mentioned in the Section S4 in the Supporting Information, using 2-amino pyridine in 100 mM H_2SO_4 as a standard [33]. Ag-NPs showed an excellent quantum yield of about 45%. At last, the fluorescence of Ag-NPs was measured using different excitation wavelengths, and it did not show any dependence of the fluorescence maxima on the excitation wavelength (**Fig. 2E**), which demonstrates the presence of a sole fluorophore with a narrow size range, proofing the quality of the synthesized Ag-NPs.

The elemental composition of Ag-NPs was also investigated using EDX spectroscopy, which revealed silver absorption peaks at 3 KV that supported the formation of Ag-NPs **(Fig. 2F)**. It's possible that the C, O, Cl, and K peaks that also showed up were caused by the *Tailed Peeper* extract.

3.2. Application of silver nanoparticles (Ag-NPs) as a self-ratiometric probe for vanillin determination

The synthesized Ag-NPs have λ_{em} at 360 nm and shoulder peak at 430 nm after excitation at λ_{ex} of 265 nm. A self-ratiometric fluorescent nanosensor for vanillin was designed using synthesized Ag-NPs based on the fluorescence quenching and redshift of Ag-NPs fluorescence peak from 360 nm to 385 nm. Upon interaction of Ag-NPs with vanillin, the fluorescence peak at 360 nm is quenched and shifted to a longer wavelength in a concentration-dependent manner till it reaches 385 nm. It is noteworthy to emphasize that the observed red shift in the fluorescence peak maxima of Ag-NPs in the presence of increasing concentrations of vanillin is a distinctive phenomenon observed in systems involving the inner filter effect (IFE). This phenomenon is commonly referred to as IFE-induced concentration-dependent redshift (CDRS). The maximum wavelength (λ_{max}) of fluorescence experiences a red shift as the concentration of vanillin is increased, primarily as a result of the enhanced IFE that occurs at these elevated concentrations. This phenomenon is widely recognized and validated in systems that involve secondary IFE. It occurs as a result of the overlap between the absorption spectrum of the quencher (vanillin) and the emission spectrum of the fluorophore (Ag-NPs), which is caused by the absorption of radiation from the shorter wavelength region of the fluorescence emission peak [34]. At the same time, the shoulder fluorescence peak of Ag-NPs at 430 nm is not significantly affected by vanillin. Consequently, the peaks at 385 nm and the shoulder peak at 430 were explored as built-in reference peaks for using the synthesized Ag-NPs as a self-ratiometric probe for vanillin determination. In this instance, the change in fluorescence ratio remains consistent because of the simultaneous increase or decrease in the fluorescence of emission bands, which lowers the detection error. This allowed for their efficient application as a ratiometric fluorescent nanosensor for the determination of vanillin. Since the signal is normalized in this

instance by the ratiometric measurements, the analysis is less prone to potential interferences from different sources of variation, such as fluctuations in the excitation source. As a result, the ratiometric fluorescence approach, like the internal standard method used in several other analytical methods, benefits from internal calibration, providing more accurate quantification than FI-based assays.

In the proposed ratiometric approach, the fluorescence intensity at 385 or 430 nm (reference peaks) is divided by the fluorescence intensity at 360 nm, and the resulting ratio is plotted versus the concentration of vanillin to construct the calibration plot. At first, the experimental conditions were optimized to get the maximum fluorescence quenching of Ag-NPs by vanillin. The effect of the pH of the reaction medium on vanillin's ability to quench the fluorescence of Ag-NPs was examined over the pH range of 2–12 using the Britton–Robinson buffer. It was demonstrated that the fluorescence quenching of Ag-NPs by vanillin increased as the pH increased until it reached a fixed value at pH 10 (**Fig. S1A**), which was selected for the next experiments. Furthermore, the buffer volume was studied using volumes ranging from 0.5 mL to 2.0 mL. The results revealed that 1.0 mL was the optimum buffer volume for the next experiments **(Fig. S1A)**. The incubation time effect on quenching of the FI of Ag-NPs by vanillin was studied at different time intervals from 1 – 60 min. It was found that quenching of the fluorescence intensity was instantaneous and remained stable for about 60 min **(Fig. S1B)**, allowing the development of a mix and measure strategy for vanillin determination.

Next, to construct the calibration plot for vanillin, different concentrations of vanillin (0-8.0 µg/mL) were mixed with Ag-NPs and the fluorescence spectra were recorded after excitation at 265 nm (**Fig. 3A**). The ratios of FI_{385}/FI_{360} and FI_{430}/FI_{360} were plotted against vanillin concentrations (**Figs. 3B, C**) to build the two calibration plots for vanillin using the FI at 430 nm and 385 nm as dual self-reference. For comparison purposes, three more calibration plots were constructed by plotting FI_0/FI_S, FI_0-FI_S, or FI_S *versus* vanillin concentrations where FI_0 is blank Ag-NP fluorescence intensity at 360 nm and FI_S is Ag-NP FI at 360 nm in the presence of the sample containing vanillin, and the results are shown in **Fig. S2** (Supplementary material). As can be seen in the calibration plots (**Figs. 3B, C** and **Fig. S2**), the correlation coefficient was very good using FI_{385}/FI_{360} and FI_{430}/FI_{360} as response having a coefficient of determination of 0.9944 and 0.9912 (**Figs. 3B, C**), respectively, while upon using the classical non-ratiometric response FI_0/FI_S, the coefficient of determination decreased to below 0.99 (**Fig. S2A**). Additionally, when FI_0-FI_S, and FI_S were used as responses, the coefficient of determination was less than 0.95 (**Fig. S2B, C**). It is concluded that the innovative

ratiometric probe significantly improved the linearity of the analytical response. The best results were obtained using FI_{385}/FI_{360} as the analytical response (**Fig. 3B**), and it was adopted in further studies.

3.3. Validation of silver nanoparticles (Ag-NPs) as a self-ratiometric probe for vanillin determination

The proposed method was validated according to ICHQ2 (R1) guidelines [23]. As shown in **Fig. 3B**, the method was linear within the concentration range of 0.05 to 8.0 µg/mL, and the LOD (3.3 SD/Slope) and the LOQ (10 SD/Slope) [23] were found to be 0.009 and 0.027, respectively, where SD is the blank standard deviation and b is the slope of the regression line. The regression equation was found to be y = 0.169 x + 0.616 with a correlation coefficient (r) of 0.997.

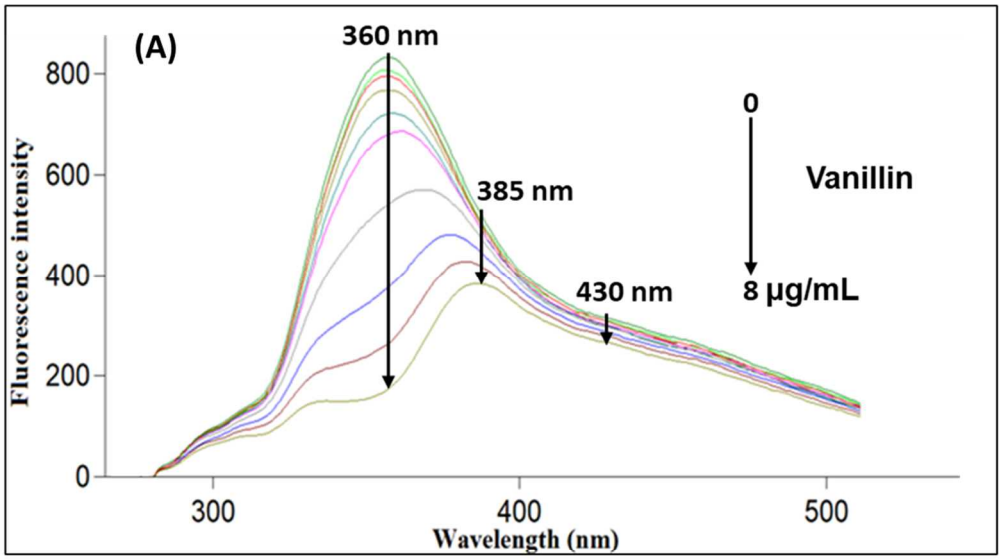

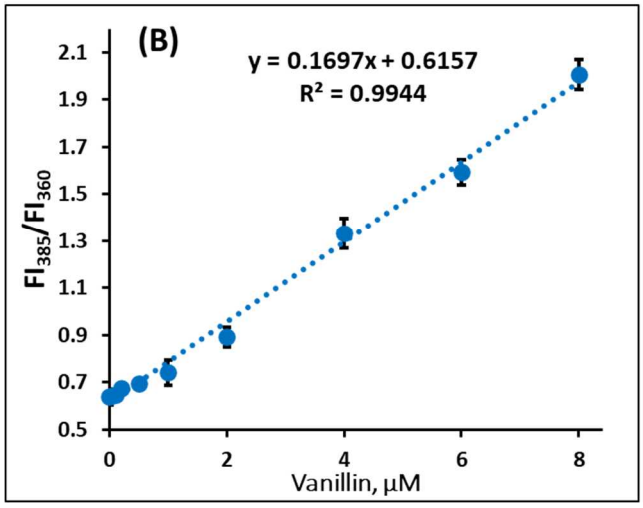

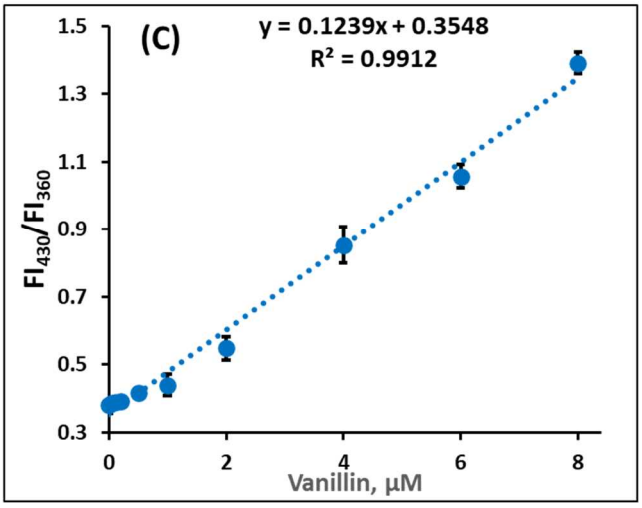

Fig. 3. (A) The fluorescence spectra of Ag-NPs upon addition of different vanillin concentrations from 0 to 8.0 µg/mL, (B) and (C) shows the calibration plots of vanillin through plotting of FI_{385}/FI_{360} and FI_{430}/FI_{360}, respectively on the y-axis vs. vanillin concentrations (µg/mL) on the x-axis.

The method's accuracy was evaluated using the mean percent found and tested in triplicate runs with varied concentrations covering the linearity range **(Table S1)**. High recovery percentages (98.60–101.90%) were obtained, demonstrating the method's high accuracy.

In addition, inter-day and intra-day precisions were investigated at three concentration levels of vanillin (0.2, 4.0, and 6.0 µg/mL) and presented as % RSD and % error. The cited analyte, vanillin, had low % RSD values (≤ 1.34%) and % error (≤ 0.77%), indicating that the developed approach was reasonably precise **(Table S2)**.

To rule out the possibility of interference and confirm the method's selectivity, the effects of different metal ions, including Mg^{+2}, Ba^{+2}, Ca^{+2}, Na^{+}, and K^{+} were thoroughly examined. As metals are present in milk and plasma samples [35], their interference was studied to confirm that they did not interfere with vanillin determination in those matrices. Also, metals are well-known interferent for nanomaterials fluorescence [36]. The effect of excipients was also studied, including maltose, lactose, dextrin, glucose, and citric acid. The selectivity study was extended to include the chemically related species, amino acids such as glutathione and cysteine, polyhydroxy compounds such as mannitol, as well as urea, uric acid, and ascorbic acid. The interference test was executed under optimum conditions in the presence of 100-fold concentrations of these disruptors to vanillin (8.0 µg/mL). All the studied disruptors had no impact on the Ag-NP ratiometric response (**Fig. 4**). These results demonstrate the potential applicability of the developed method for measuring vanillin in milk formula, biscuits, and plasma samples with suitable selectivity.

All the studied disruptors had no impact on the Ag-NP ratiometric response. These results demonstrate the potential applicability of the developed method for measuring vanillin in milk formula, biscuits, and plasma samples with suitable selectivity.

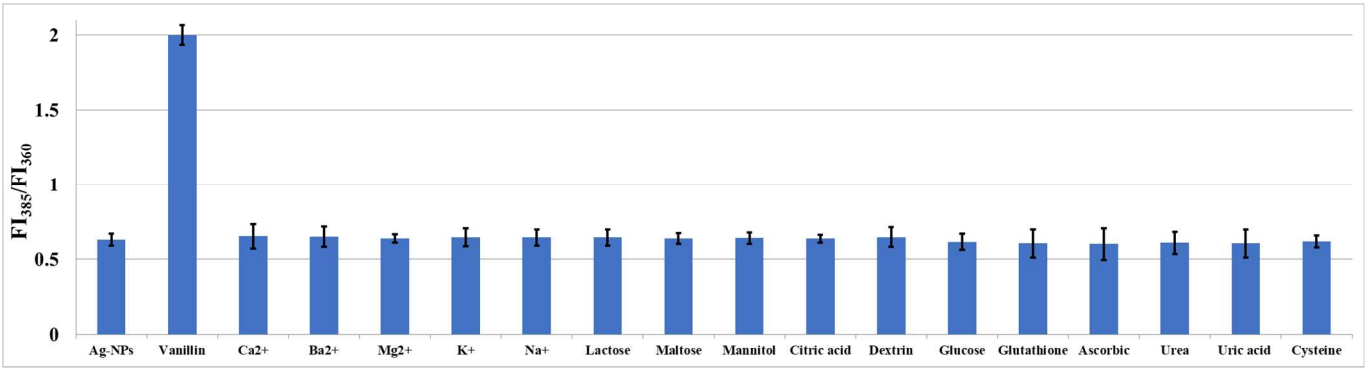

Fig. 4. The selectivity of Ag-NPs towards vanillin (8.0 µg/mL) in the presence of 100-fold of possible interfering disruptors, including metals, sugars, amino acids, and polyhydroxy compounds.

3.4. Mechanism of fluorescence quenching

Fluorescence quenching typically occurs through various mechanisms, including the inner filter effect (IFE), dynamic quenching, static quenching, photo-induced electron transfer (PET), intramolecular charge transfer (ICT), or fluorescence resonance energy transfer (FRET) [37]. IFE happens when the quencher absorbs either the excitation or the emission light. IFE is typically a troublesome source in spectrofluorimetry studies, but recent research has shown that it can be used to create novel fluorescence assays [32]. In the present study, the IFE was predicted to occur because there is an overlap between the emission spectra of the Ag-NPs (the fluorophore) and the UV-visible absorption spectra of vanillin (the quencher) **(Fig. 5A).**

After adding vanillin, the FI of Ag-NP's fluorescence was corrected by subtraction of IFE using equation **(1)**: $\mathbf{F_{corr} = F_{obs} \times 10^{(A_{ex} + A_{em})/2}}$ **(1)**

Where: A_{ex} and A_{em} refer to the drug absorbance at the excitation and emission wavelengths, respectively. F_{corr} and F_{obs} refer to the fluorescence intensity corrected and observed after excluding the IFE from the F_{obs}.

Equation (2) was used to calculate the suppressed efficiency (%E) for both the corrected and observed fluorescence:

$$\mathbf{\%E = [1 - (F/F_0)] \times 100} \quad \mathbf{(2)}$$

Where: F_0 is the blank FI, F is the F_{corr} or F_{obs}, and % E is the suppressed efficiency.

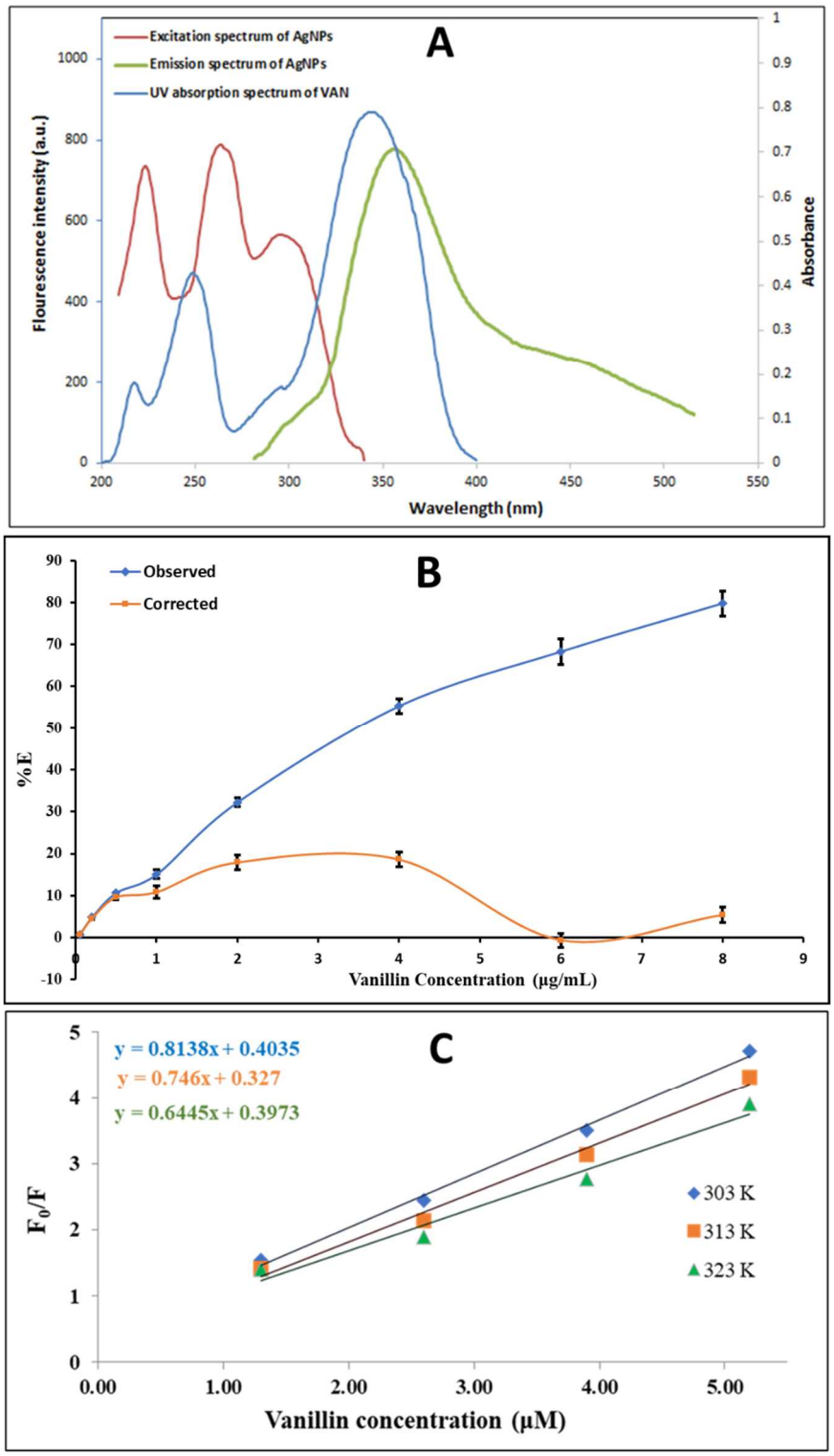

Fig. 5. Results of the study of the quenching mechanism of vanillin on Ag-NP's fluorescence. Where (**A**) A co-plot displaying the fluorescence excitation and emission spectrum of Ag-NPs and the UV-Vis absorption spectrum of vanillin showing the great overlap between the emission of the AgNPs and the UV spectra of vanillin, (**B**) The quenching efficiency (% E) using corrected and observed fluorescence of Ag-NPs in the presence of different concentrations of vanillin (0.05-8.0 µg/mL), and **(C)** Stern-Volmer plots for vanillin as a quencher for Ag-NP's fluorescence at 303, 313, and 323 K.

Fig. 5B shows a plot of the %E of the corrected and observed fluorescence intensities of Ag-NPs against vanillin concentrations in µg/mL. It is revealed that the IFE is the main mechanism for quenching Ag-NP's fluorescence by vanillin. The contribution of other quenching mechanisms, including static and dynamic quenching, was studied using Stern-Volmer analysis at different temperatures (**Fig. 5C**). It was found that the Stern-Volmer constant (K_{SV}) decreased by raising the temperature, demonstrating the static quenching serves as an additional quenching mechanism in addition to the IFE [38]. For more details about the performed Stern-Volmer analysis, please refer to Supporting Information Section S5.

3.5. Application of the designed ratiometric probe for the determination of vanillin in food products and plasma

In silico toxicological evaluation of vanillin *via* the admetSAR (V 2.0) program [39] revealed its potential as a harmful substance to the kidneys, liver, and reproductive system. The *Tetrahymena pyriformis* toxicity model and the fish aquatic toxicity model both classify it as a toxic substance. Vanillin's potential genotoxicity was determined by the built-in model, which is based on a sizable database of results from *in vivo* micronucleus assays. Vanillin can inhibit OATP1B1 and OATP1B3, which are organic anion-transporting polypeptide hepatic proteins. As a result, it might play a part in drug-drug interactions after exposure. Therefore, it is essential to develop a new, quick, and accurate analytical technique to detect vanillin in various food samples, particularly infant formula and meals.

Hence, our method was applied to determine vanillin in different adult and infant foods and milk formula samples. Especially considering the prohibition of vanillin in infant baby formula below six months old. The % recoveries of spiked vanillin in milk formula samples ranged from 95.39–102.67%, while in biscuits, samples ranged from 95.28–104.29% **(Table 1)**. The obtained good recoveries%, together with the low percent RSD values (≤ 3.85%) without interference, demonstrated the good applicability and the suitable selectivity of the proposed approach for the determination of vanillin in such matrices **(Table 1)**.

Table 1. Results for utilizing the suggested technique for determination of vanillin in real milk formula and food samples.

Sample	The amount added (µg/mL)	The amount found (µg/mL)	% Recovery[a]	% RSD (n = 3)
Infant milk formula	-	-	-	-
	2.0	1.91	95.50	3.28
	4.0	4.06	101.5	2.75
	6.0	6.16	102.7	1.94
	8.0	7.87	98.38	2.62
Biscuit	-	-		-
	2.0	2.09	104.5	1.88
	4.0	4.01	100.3	3.85
	6.0	5.71	95.17	2.49
	8.0	8.19	102.4	1.65

[a]Each result is an average of 3 separate determinations (n = 3).

The method applicability was also extended to determine vanillin in spiked human plasma samples with selectivity without interference from the endogenous plasma components. The method exhibited high % recoveries (97.15–104.64%) and low % RSD values (≤ 3.301%), as presented in **Table 2**. Furthermore, absolute recovery for the plasma extraction method was determined by comparing standards prepared in blank plasma to standards prepared in distilled water, and it was found to be 99.0% on average, demonstrating the excellent performance of the extraction method.

Table 2. Results for utilizing the suggested technique for determination of vanillin in spiked human plasma.

Parameter	Conc. Taken (µg/mL)	Conc. Found (µg/mL)	% Recovery[a]
	2.0	2.09	104.50
	4.0	3.95	98.75
	6.0	5.83	97.17
	8.0	8.13	101.6
Mean			100.51
± SD			3.23
% RSD			3.22
% Error			1.62

[a]Each result is the average of 3 separate determinations (n = 3).

4. Greenness and whiteness profile of the developed self-ratiometric method

The developed analytical method underwent a rigorous green and sustainability evaluation, meticulously assessing each step involved. At first, the Spider Diagram tool was utilized, which provided a greenness index for the used chemicals based on safety data sheets (SDSs) information, enabling the assessment of the solvents' sustainability [24]. Furthermore, applying the AGREE tool [25] and the RGB12 [28] was helpful in evaluating each step's environmental impact and

sustainability in the analytical procedure. Furthermore, utilizing the AGREEprep tool [26] enabled the valuation of sample preparation methods greenness. Furthermore, pre-analysis steps such as preparing the *Tailed pepper* extract and synthesizing Ag-NPs underwent evaluation using the ComplexGAPI tool [27]. The utilization of multiple evaluation tools enabled a comprehensive assessment of the analytical procedure's adherence to the 12 concepts of Green Analytical Chemistry (GAC) [28] and the 12 sustainability principles, commonly known as the 12 White Analytical Chemistry guidelines (WAC). Integrating multiple evaluation tools is essential in obtaining a thorough and scientifically rigorous evaluation of the proposed analytical procedure's greenness and sustainability [40]. The developed self-ratiometric fluorescent nanosensor ensures adhering to all the green and sustainable analytical chemistry ideologies, promotes sustainability, and aligns with the principles of green sample preparation. For a detailed explanation, please refer to supplementary Information Section S5.

5. Comparison of the performance of the developed method and reported literature for measurement of vanillin additive in infants' and adults' foods and/or biological fluids.

The performance of the synthesized Ag-NP ratiometric fluorescence probe as a nanosensor for determining vanillin in various matrices was compared with the previously reported methods for vanillin determination, and the comparison is illustrated in **Table 3**. The developed sensor has excellent sensitivity with a LOD of 0.01µg/mL. This LOD is 21 to 138 times more sensitive than the previously reported fluorescence sensors [5–7], 16 to 23 times more sensitive than most of the previously reported electrochemical probes [9–11], comparable sensitivity to the Au–Ag alloy nanoparticles voltammetric method [12], and 14 times more sensitive than the recently reported chemiluminescence method [16] for vanillin determination. Our method showed comparable sensitivity to the graphene quantum dot fluorometric method; however, we provided a ratiometric probe that was synthesized in a shorter time and provided better precision [8]. Apart from sensitivity, the previously reported fluorimetric methods [5–7] used metal-based organic fluorophores that require sophisticated synthesis and are harmful to the environment. In addition, most of the reported electrochemical methods require the laborious preparation of specially modified electrodes, limiting their widespread use. Besides, the turnaround time of the previously reported methods is quite long. Furthermore, there is no reference value to correct run-to-run drifts in these methods. On the other hand, our probe was synthesized from cost-effective natural substrates, using rapid one-pot microwave synthesis within less than one minute. Moreover, our developed sensor is a self-ratiometric probe that self-corrects the erroneous difference between measurements and can eliminate several interferent effects.

For evaluation of the ecological implication of the developed ratiometric method, its whiteness was evaluated using the RGB12 tool and then compared with the whiteness of previously reported methods for vanillin. The evaluation results of reported methods for vanillin determination are depicted in **Fig. S3** and **Fig. S4**. The presented data reveals that the overall assessments exhibited relatively similar results, ranging from 81.1% (as reported in *T. Shao et al.'s* method [16] to 99.2% (in the developed method). This indicates that the analyzed methods possess comparable overall potential. However, upon meticulous examination of the contribution of each primary colour, our developed ratiometric method has an impressive R (%) value of 107.5%, while G (%) and B (%) achieved a noteworthy 95.0%. This remarkable equilibrium among the three primary attributes led to a significantly high whiteness value, nearing perfection at nearly 100%. The developed ratiometric sensor demonstrated high sensitivity and the ability to analyze minute concentrations of samples containing vanillin. This was evident in the exceptional scores for red principles, surpassing 100.

Table 3. Comparison of the performance of the developed nanosensor for vanillin with the previously reported ones in the literature.

Method	**Sensor**	**Sample**	**Linearity range** µg/mL	**% Recovery**	**Turn around time**	**% RSD**	**LOD (µg/mL)**	**Ref**
Fluorimetry	Luminescent Cd(II) coordination polymer	Infant formula	NA	95.2 - 106.9%	> 4 days	NA	0.21	[5]
Fluorimetry	CdSe/ZnS quantum dots	Sugar, milk, and custard	2.0-20.0	90-105%	45 min - 4 hours	4.1	0.99	[6]
Fluorimetry	Co(II)-based MOFs nanoflakes	Milk powders	10.7-22.8	99.89 - 100.06 %	> 22 hours	≤ 0.5	1.38	[7]
Fluorimetry	Graphene quantum dots	Chocolate samples	0-3.0	88.0-108.9%	44 min	5.4	0.004	[8]
Voltammetry	Multiwalled carbon nanotube screen-printed electrode	Natural Vanilla	0.4-114.1	NA	8 minutes	NA	0.16	[9]
Voltammetry	Anodically pretreated boron-doped diamond electrode	Vanilla sugar, foamy instant coffee, and cola soft drink	2.5-150.0	92.32 - 97.63%	2.5 hours	5.7	0.23	[10]
Voltammetry	Ionic surfactant-modified graphene paste electrode	Biscuit and beverage	3.0 – 10.6	94.25-107%	20 min	3.2	0.20	[11]
Voltammetry	Au–Ag alloy nanoparticles	Bean and tea	0.03-7.6	96.3-103.4%	12 h	7.9	0.006	[12]
Chemi-luminescence	Luminol-H_2O_2 and β-cyclodextrin	Milk powder and biscuits	0.15-16.7	101.59-109.56%	30 min	≤ 8.5	0.14	[16]

Fluorimetry	Nanomaterials (Ag-NPs ratiometric fluorescence system)	Infant milk formula, biscuits, & plasma samples	0.05 - 8.0	95.3-104.6%	40 sec	≤ 1.3	0.009	The proposed method

6. Method's limitations and challenges

Working in the UV region ($\lambda_{excitation}$ = 265 nm) makes the probe prone to interferences by biomatter. Blood, serum, cells, marine water, wastewaters, etc., always display strong background UV absorption and fluorescence. The UV light used for fluorescence excitation could be screened off by UV absorbers, and this will weaken the signal, and the same could happen to emitted UV fluorescence. In the current study, the developed probe did not suffer from these interferences, and very good recovery results (95.3-104.6%) were obtained. This could be attributed to the self-ratiometric nature of the probe, which corrects any interference. The UV absorbing compounds may affect the fluorescence intensity at 360 nm, but they will affect the fluorescence intensity at 385 nm similarly, and the ratio will remain unchanged at the end. This is the main advantage of using a self-ratiometric probe, which allows overcoming this issue.

7. Conclusion

The current study provides a novel built-in ratiometric fluorescent nanosensor using green-biosynthesized Ag-NPs for the sensitive and selective determination of vanillin in adult and infant foods and milk formulas. Ag-NPs have been synthesized using a straightforward green microwave-assisted method that uses *Tailed pepper* seed extract as a reducing agent. In the proposed ratiometric probe, the fluorescence intensity ratio of Ag-NP/vanillin system FI_{385}/FI_{360} was used as the analytical response ratio that was plotted *versus* the concentration of vanillin to construct the calibration plots. The developed ratiometric probe was successfully applied for the determination of vanillin in milk formula and biscuit samples with high percentage recoveries and low percentage RSD values. The proposed approach was also used to determine vanillin in spiked human plasma samples. Multiple metrics, including the spider diagram, AGREE, AGREEprep, Complex-GAPI, and RGB12, were applied to assess the greenness and whiteness of the proposed and reported methods for vanillin determination. By employing these diverse greenness and whiteness metrics, a comprehensive profile of greenness and sustainability can be obtained, providing valuable insights to analysts and identifying areas for improvement in analytical approaches. The main challenge for the designed probe was using an excitation wavelength in the UV region ($\lambda_{excitation}$ = 265 nm), which could make

the probe prone to interferences by biomatter, but this issue was resolved by the self-ratiometric nature of the probe, which corrected any potential interference.

Funding: This research work was funded through project number SU-ANN-202218, provided by the deanship of scientific research at the College of Pharmacy, Shaqra University, Shaqra, Saudi Arabia.

Competing Interest declaration: The authors declare that they have no known competing financial interests or personal relationships that could have appeared to influence the work reported in this paper.

References

1. WHO (2004) Evaluation of certain food additives and contaminants: eightieth report of the Joint FAO/WHO Expert Committee on Food Additives
2. Deng P, Xu Z, Zeng R, Ding C (2015) Electrochemical behavior and voltammetric determination of vanillin based on an acetylene black paste electrode modified with graphene–polyvinylpyrrolidone composite film. Food Chem 180:156–163. https://doi.org/10.1016/j.foodchem.2015.02.035
3. Barghini P, Di Gioia D, Fava F, Ruzzi M (2007) Vanillin production using metabolically engineered Escherichia coli under non-growing conditions. Microb Cell Fact 6:13. https://doi.org/10.1186/1475-2859-6-13
4. Ni Y, Zhang G, Kokot S (2005) Simultaneous spectrophotometric determination of maltol, ethyl maltol, vanillin and ethyl vanillin in foods by multivariate calibration and artificial neural networks. Food Chem 89:465–473. https://doi.org/10.1016/j.foodchem.2004.05.037
5. Chen Y, Liu G, Lu X, Wang X (2022) A water-stable new luminescent Cd(II) coordination polymer for rapid and luminescent/visible sensing of vanillin in infant formula. Inorganica Chim Acta 540:121051. https://doi.org/10.1016/j.ica.2022.121051
6. Durán GM, Contento AM, Ríos Á (2015) β-Cyclodextrin coated CdSe/ZnS quantum dots for vanillin sensoring in food samples. Talanta 131:286–291. https://doi.org/10.1016/j.talanta.2014.07.100
7. Wang J, Ni Y (2020) Ammonium molybdate-assisted shape-controlled synthesis of fluorescent Co(II)-based MOFs nanoflakes as highly-sensitive probes for selective detection of vanillin in milk powders. Mater Res Bull 123:110721. https://doi.org/10.1016/j.materresbull.2019.110721
8. Zhu S, Bai X, Wang T, et al (2021) One-step synthesis of fluorescent graphene quantum dots as an effective fluorescence probe for vanillin detection. RSC Adv 11:9121–9129. https://doi.org/10.1039/D0RA10825A
9. Chen L, Chaisiwamongkhol K, Chen Y, Compton RG (2019) Rapid Electrochemical Detection of Vanillin in Natural Vanilla. Electroanalysis 31:1067–1074. https://doi.org/10.1002/elan.201900037
10. Ali HS, Abdullah AA, Pınar PT, et al (2017) Simultaneous voltammetric determination of vanillin and caffeine in food products using an anodically pretreated boron-doped diamond

electrode: Its comparison with HPLC-DAD. Talanta 170:384–391. https://doi.org/10.1016/j.talanta.2017.04.037

11. Raril C, Manjunatha JG (2020) A simple approach for the electrochemical determination of vanillin at ionic surfactant modified graphene paste electrode. Microchem J 154:104575. https://doi.org/10.1016/j.microc.2019.104575

12. Zheng D, Hu C, Gan T, et al (2010) Preparation and application of a novel vanillin sensor based on biosynthesis of Au–Ag alloy nanoparticles. Sensors Actuators B Chem 148:247–252. https://doi.org/10.1016/j.snb.2010.04.031

13. Minematsu S, Xuan G-S, Wu X-Z (2013) Determination of vanillin in vanilla perfumes and air by capillary electrophoresis. J Environ Sci 25:S8–S14. https://doi.org/10.1016/S1001-0742(14)60617-3

14. Takahashi M, Sakamaki S, Fujita A (2013) Simultaneous Analysis of Guaiacol and Vanillin in a Vanilla Extract by Using High-Performance Liquid Chromatography with Electrochemical Detection. Biosci Biotechnol Biochem 77:595–600. https://doi.org/10.1271/bbb.120835

15. De Jager LS, Perfetti GA, Diachenko GW (2008) Comparison of headspace-SPME-GC–MS and LC–MS for the detection and quantification of coumarin, vanillin, and ethyl vanillin in vanilla extract products. Food Chem 107:1701–1709. https://doi.org/10.1016/j.foodchem.2007.09.070

16. Shao T, Song X, Jiang Y, et al (2023) Vanillin-Catalyzed highly sensitive luminol chemiluminescence and its application in food detection. Spectrochim Acta Part A Mol Biomol Spectrosc 294:122535. https://doi.org/10.1016/j.saa.2023.122535

17. El-Maghrabey MH, Nakatani T, Kishikawa N, Kuroda N (2018) Aromatic aldehydes as selective fluorogenic derivatizing agents for α-dicarbonyl compounds. Application to HPLC analysis of some advanced glycation end products and oxidative stress biomarkers in human serum. J Pharm Biomed Anal 158:38–46. https://doi.org/10.1016/j.jpba.2018.05.012

18. Yan H, Sun Z, Qing M, et al (2023) Kill two birds with one stone: Ratiometric sensing of phosphate via a single-component probe with fluorescence-scattering dual-signal response behavior. Anal Chim Acta 1246:340866. https://doi.org/10.1016/j.aca.2023.340866

19. El-Maghrabey M, El-Shaheny R, Belal F, et al (2020) Green Sensors for Environmental Contaminants. In: Inamuddin M, Asiri A (eds) Nanosensor Technologies for Environmental Monitoring. Nanotechnology in the Life Sciences. Springer, Cham, pp 491–516

20. Mittal AK, Chisti Y, Banerjee UC (2013) Synthesis of metallic nanoparticles using plant extracts. Biotechnol Adv 31:346–356. https://doi.org/10.1016/j.biotechadv.2013.01.003

21. Ahmad S, Munir S, Zeb N, et al (2019) Green nanotechnology: a review on green synthesis of silver nanoparticles — an ecofriendly approach. Int J Nanomedicine Volume 14:5087–5107. https://doi.org/10.2147/IJN.S200254

22. Ratan ZA, Haidere MF, Nurunnabi M, et al (2020) Green Chemistry Synthesis of Silver Nanoparticles and Their Potential Anticancer Effects. Cancers (Basel) 12:855. https://doi.org/10.3390/cancers12040855

23. International Conference on Harmoanization (2005) Validation of analytical procedures: text and methodology, Q2(R1). Geneva

24. Shen Y, Lo C, Nagaraj DR, et al (2016) Development of Greenness Index as an evaluation tool to assess reagents: Evaluation based on SDS (Safety Data Sheet) information. Miner Eng 94:1–9. https://doi.org/10.1016/j.mineng.2016.04.015

25. Pena-Pereira F, Wojnowski W, Tobiszewski M (2020) AGREE—analytical greenness metric approach and software. Anal Chem 92:10076–10082. https://doi.org/10.1021/acs.analchem.0c01887

26. Wojnowski W, Tobiszewski M, Pena-Pereira F, Psillakis E (2022) AGREEprep – Analytical greenness metric for sample preparation. TrAC Trends Anal Chem 149:116553. https://doi.org/10.1016/j.trac.2022.116553

27. Płotka-Wasylka J, Wojnowski W (2021) Complementary green analytical procedure index (ComplexGAPI) and software. Green Chem 23:8657–8665. https://doi.org/10.1039/D1GC02318G

28. Nowak PM, Wietecha-Posłuszny R, Pawliszyn J (2021) White Analytical Chemistry: An approach to reconcile the principles of Green Analytical Chemistry and functionality. TrAC Trends Anal Chem 138:116223. https://doi.org/10.1016/j.trac.2021.116223

29. Shang L, Zhao F, Zeng B (2014) Sensitive voltammetric determination of vanillin with an AuPd nanoparticles−graphene composite modified electrode. Food Chem 151:53–57. https://doi.org/10.1016/j.foodchem.2013.11.044

30. Qiang LS, Rukayadi Y, Padzil KNM, Razis AFA (2022) Antioxidant activity of Piper cubeba L. berries crude extracts and its fractions. Food Res 6:279–286. https://doi.org/10.26656/fr.2017.6(4).611

31. Siakavella IK, Lamari F, Papoulis D, et al (2020) Effect of Plant Extracts on the Characteristics of Silver Nanoparticles for Topical Application. Pharmaceutics 12:1244. https://doi.org/10.3390/pharmaceutics12121244

32. El-Shaheny R, Al-Khateeb LA, El Hamd MA, El-Maghrabey M (2021) Correction pen as a hydrophobic/lipophobic barrier plotter integrated with paper-based chips and a mini UV-torch to implement all-in-one device for determination of carbazochrome. Anal Chim Acta 1172:338684. https://doi.org/10.1016/j.aca.2021.338684

33. Rurack K Fluorescence Quantum Yields: Methods of Determination and Standards. In: Resch-Genger U (ed) Standardization and Quality Assurance in Fluorescence Measurements I. Springer, Berlin, Heidelberg, pp 101–145

34. Qandeel NA, El-Masry AA, Eid M, et al (2023) Fast one-pot microwave-assisted green synthesis of highly fluorescent plant-inspired S,N-self-doped carbon quantum dots as a sensitive probe for the antiviral drug nitazoxanide and hemoglobin. Anal Chim Acta 1237:340592. https://doi.org/10.1016/j.aca.2022.340592

35. Pereira JSF, Pereira LSF, Schmidt L, et al (2013) Metals determination in milk powder samples for adult and infant nutrition after focused-microwave induced combustion. Microchem J 109:29–35. https://doi.org/10.1016/j.microc.2012.05.010

36. Cai L, Fu Z, Cui F (2020) Synthesis of Carbon Dots and their Application as Turn Off–On Fluorescent Sensor for Mercury (II) and Glutathione. J Fluoresc 30:11–20. https://doi.org/10.1007/s10895-019-02454-5

37. Zu F, Yan F, Bai Z, et al (2017) The quenching of the fluorescence of carbon dots: A review on mechanisms and applications. Microchim Acta 184:1899–1914. https://doi.org/10.1007/s00604-017-2318-9

38. Magdy G, Abdel Hakiem AF, Belal F, Abdel-Megied AM (2021) Green one-pot synthesis of nitrogen and sulfur co-doped carbon quantum dots as new fluorescent nanosensors for determination of salinomycin and maduramicin in food samples. Food Chem 343:128539. https://doi.org/10.1016/j.foodchem.2020.128539

39. Cheng F, Li W, Zhou Y, et al (2012) admetSAR: A comprehensive source and free tool for assessment of chemical ADMET properties. J Chem Inf Model 52:3099–3105. https://doi.org/10.1021/ci300367a

40. El Hamd MA, El-Maghrabey M, Magdy G, et al (2023) Application of quality-by-design for adopting an environmentally green fluorogenic determination of benoxinate hydrochloride in eye drops and artificial aqueous humour. Sci Rep 13:8559. https://doi.org/10.1038/s41598-023-35347-6

SUPPLEMENTARY INFORMATION (SI)

Section S1: Instrumentation

Cary Eclipse Fluorescence Spectrophotometer (Agilent Technologies, United States) was used to measure the fluorescence using a Xenon flash lamp. The slit width was set to 5 nm, and the adjustment of voltage was to 800 V. The spectrophotometric measurements were conducted using a double-beam spectrophotometer (PG Instrument, UK). A household microwave (Fresh, FMW-25KC-S, 900 watts) was used. A Fourier Transform Infrared (FT-IR) spectrophotometer (IS10 Nicolet, USA) was used, and all measurements were made between 4000 and 1000 cm^{-1} as 32 scans at a resolution of 4 cm^{-1}. A JEOL high-resolution transmission electron microscope (HRTEM) operated at 200 kV (JEM-2100, Tokyo) was used to examine the morphology of Ag-NPs. Centrifuge, model 2-16P (Germany), pH-meter (Jenway 3510, UK), SS 101H 230 ultrasonic bath (USA), and IVM-300p vortex mixer (Taiwan) were used.

Section S2: Materials and reagents

Vanillin (99%) was obtained from Lanxess AG, Colonge, Germany. Vanillin-containing foods and milk formulae were purchased from a local supermarket and pharmacy, respectively. The seeds for the *Tailed pepper* were purchased from a local herbal market. Kafrelsheikh University Hospitals (Kafrelsheikh, Egypt) donated human plasma samples frozen at -80 °C until used. Sigma-Aldrich (St. Louis, MO, USA) supplied the glacial acetic acid, phosphoric acid, methanol, and silver nitrate. Fresh solutions of 0.02 M Britton-Robinson buffer, BRB, of pH 2−12 were made. The experiments were carried out using double distilled water, and all chemicals and reagents were of analytical grade.

Section S3: Standard solutions

In ethanol, the standard vanillin solution (100.0 µg/mL) was made. Working solutions between 0.05 and 8.0 µg/mL were created by serially diluting the standard solution in double distilled water. When kept at 4 °C, the standard solution remained stable for at least a week.

Section S4: Fluorescence quantum yield measurements

The following equation was used to calculate the quantum yield of Ag-NPs [1]:

$$\Phi_{Ag\text{-}NPs} = \Phi_{St} \times (F_{Ag\text{-}NPs} / F_{St}) \times (A_{St} / A_{Ag\text{-}NPs}) \times (\eta_{Ag\text{-}NPs} / \eta_{St})^2$$

Where Φ: quantum yield, F: integrated fluorescence intensity, A: absorbance at 265 nm, and η: solvent refractive index. The used standard was 2- amino pyridine prepared in 100 mM sulfuric acid, and its Φ_{St} = 0.6. In order to decrease the inner filter effect, the measured Ag-NPs and 2- amino pyridine solutions were diluted in order to have absorbance < 0.1.

Section S5: Study of the quenching mechanism using Stern Vomer analysis

Other mechanisms, such as static or dynamic quenching, might be present beside the IFE. Static quenching results from the formation of a ground state complex. In contrast, the quencher diffuses to the fluorophore while it is excited and collides during dynamic quenching. The temperature dependence of the two suggested mechanisms is another distinction that distinguishes between them. This can be accomplished by Stern-Volmer analysis since increasing the temperature increases the value of the Stern-Volmer constant in the case of dynamic quenching while decreasing its value in the static case [2]. The possible quenching mechanisms were investigated using the Stern-Volmer Equation **(S1):**

$$F_0/F = 1 + K_{sv}[Q] = 1 + K_q\tau_0[Q] \qquad \textbf{(S1)}$$

Where: (F_0) and (F) are the fluorescence intensities before and after adding the drug, K_{SV} is the Stern-Volmer (S-V) constant, and [Q] is the concentration of quencher [3, 4].

The Stern-Volmer analysis was tested at three temperature settings (303, 313, and 323 K). F^o/F was plotted against vanillin concentration in µM using Equation **(3) (Fig. 5C).** At 303, 313, and 323 K; the K_{SV} values were 8.048×10^4, 7.3786×10^4, and 6.3741×10^4 $L.mol^{-1}$, respectively. Since K_{SV} decreased by raising the temperature, static quenching serves as an additional quenching mechanism in addition to the IFE [5]. Additionally, from the obtained K_{SV} values, k_q values were calculated and were found to be 8.048×10^{12}, 7.3786×10^{12}, and 6.3741×10^{12} $L.mol^{-1}.s^{-1}$, respectively. These

values are far larger than the maximum diffusion rate constant (2.0×10^{10} $L.mol^{-1}.s^{-1}$); further confirming the static quenching mechanism

Section S6: Greenness and whiteness profile of the developed self-ratiometric method

S6.1. Greenness solvent index via spider diagram

The assessment of reagents in the developed ratiometric fluorescent nanosensor incorporated the application of a Greenness Index evaluation tool, which was visually depicted through a spider diagram. The spider diagram visually depicted the overall sustainability level of the chemicals used and the primary spider diagram represents the greenness index for the ethanol used in preparing the standard solution is shown in **Fig. S5A**, indicating a significant safety area. The details of the spider diagram are shown in **Fig. S6**.

S6.2. AGREE tool

The AGREE software utilizes a circular pictogram resembling a clock to represent the 12 principles of GAC. Each principle is assigned a numerical value ranging from 0 to 1, indicated by a color scale from dark green to dark red. The central number in the pictogram represents the average value derived from the 12 principles. The suggested ratiometric fluorescent nanosensor method has an AGREE score of 0.61, **Fig. S5B**.

S6.3. RGB12 algorithm

This tool evaluates and categorizes the developed analytical methods based on their whiteness. These evaluations consider both productive working (represented by red and blue scores) and environmental aspects (represented by green scores). Combining these primary colors—green, red, and blue—creates white, symbolizing a sustainable analytical method. The 12 concepts of the WAC tool encompass important principles derived from GAC, validity criteria (R1-R4), and economic factors (B1-B4), as illustrated in **Fig. S5**C. The ratiometric fluorescent nanosensor achieved high greenness with a percentage close to 95.0%, attributed to the efficient use of the green solvent (ethanol) and the minimal waste generated by employing water as a diluting solvent (G1 and G2 principles). Additionally, utilizing Ag-NPs prepared from natural *Tailed Pepper* extract yielded favorable results, and the fluorimetric device exhibited high speed and low energy consumption, contributing to a blue score of approximately 95.0%. Overall, the proposed ratiometric fluorescent nanosensor obtained an excellent whiteness score, averaging around 99.2% (a combination of

predetermined RED, GREEN, and BLUE scores), indicating its sustainability. **Table S3** provides an overview of the whiteness score.

S6.4. AGREEprep tool

Furthermore, in the realm of GAC, it is crucial to emphasize the significance of sample preparation steps. The AGREEprep tool which specifically focuses on evaluating the greenness of sample preparation methods. AGREEprep considers 10 categories that align with the principles of GSP, as detailed in **Fig. S5D.** The evaluation results are visually represented by a colorful pictogram, where the final assessment value is depicted within a colored circle at the center of the pictogram. This graphical representation effectively communicates the overall greenness performance of the sample preparation process, as illustrated in **Fig. S5D**. The AGREEprep tool analysis results demonstrated environmentally friendly and sustainable practices in sample preparation for determining vanillin in the spiked human plasma and infant milk and biscuits samples within the analytical ratiometric fluorescent nanosensor.

S6.5. ComplexGAPI tool

ComplexGAPI tool covers all stages of the analytical procedure, including sample preparation, transportation, preservation, storage, and final analysis. It also considers the actions performed before using the general analytical methodology. The software assesses the green character of the suggested ratiometric fluorescent nanosensor technique and represents the results through a pictogram. The resulting color pictograph indicates the environmental consequences of each stage of the pre-analysis procedure and the analytical approach. **Fig. S5E** illustrates the ComplexGAPI pictogram for the ratiometric probe.

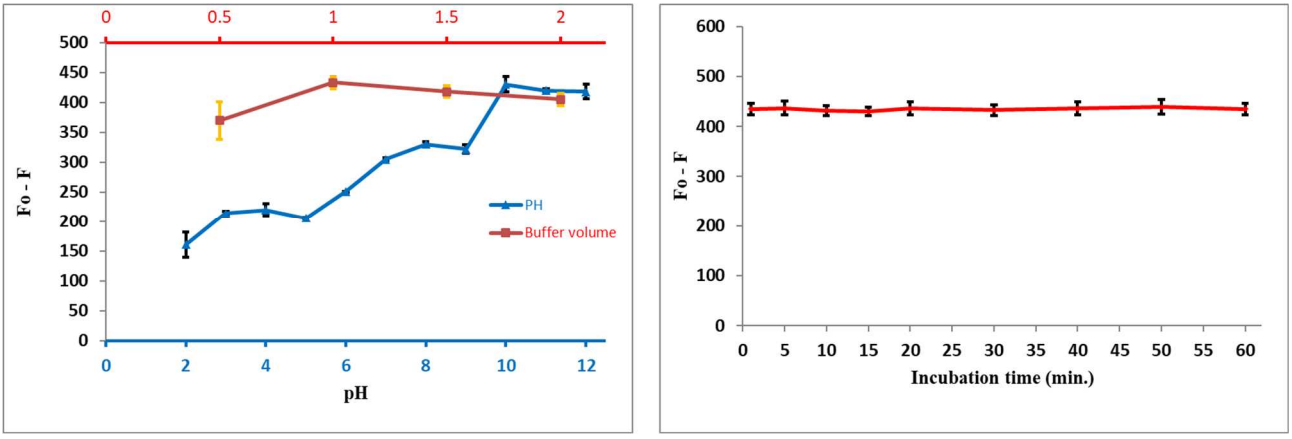

Fig. S1. Effect of the buffer pH and volume **(A)** and incubation time **(B)** on the quenching of the fluorescence spectrum of Ag-NPs by vanillin (4.0 µg/mL).

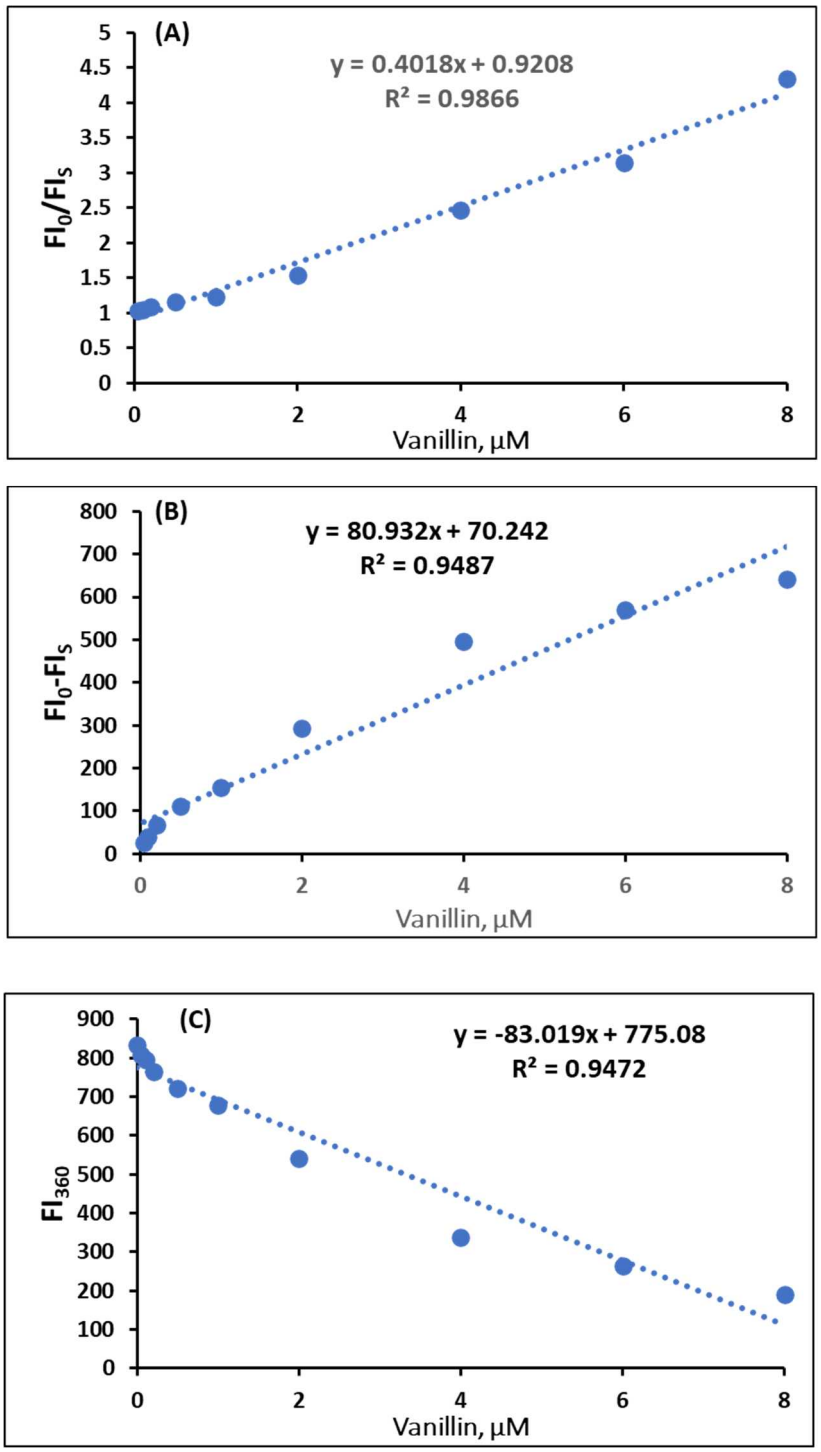

Figure S2. Calibration curves for vanillin using classical non-ratiometric responses, where (A), (B), and (C) shows the calibration curve of vanillin through plotting of FI_0/FI_S, FI_0-FI_S, and FI_S on the y-axis vs. vanillin concentrations in the x-axis, respectively.

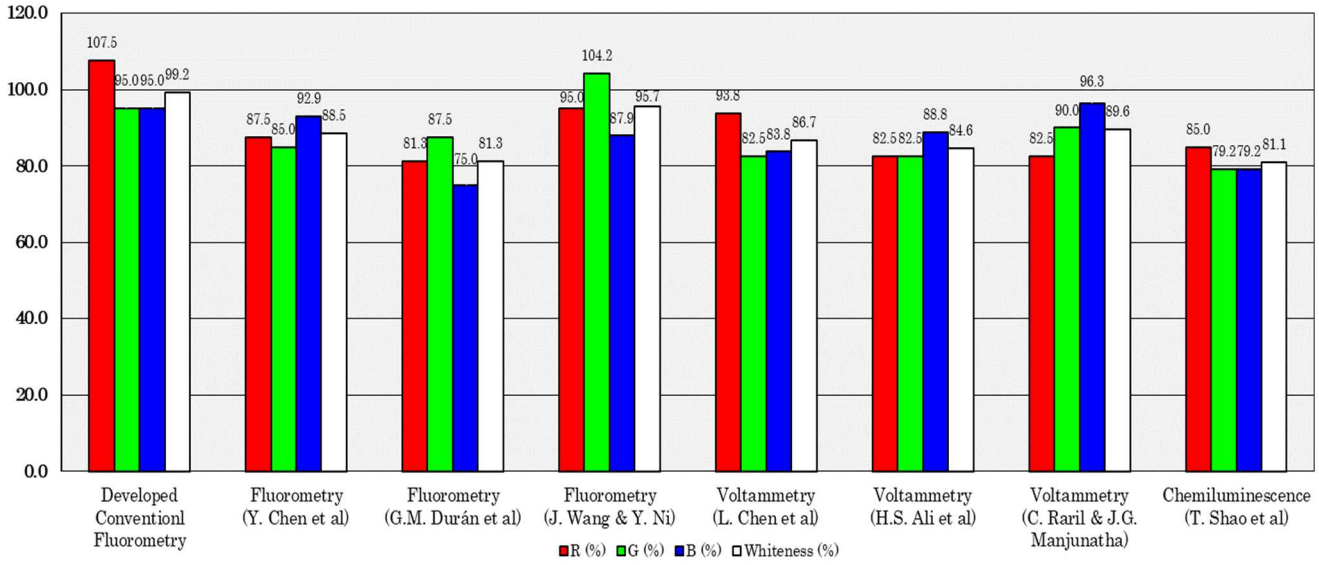

Figure S3. The assessment outcomes from the RGB 12 tool for the reported and developed methods. (Any values surpassing 100 indicate additional capabilities that go beyond the current requirements).

Figure S4. Principles of WAC and their results according to RGB12 tool for the developed and reported methods for vanillin determination in different matrices.

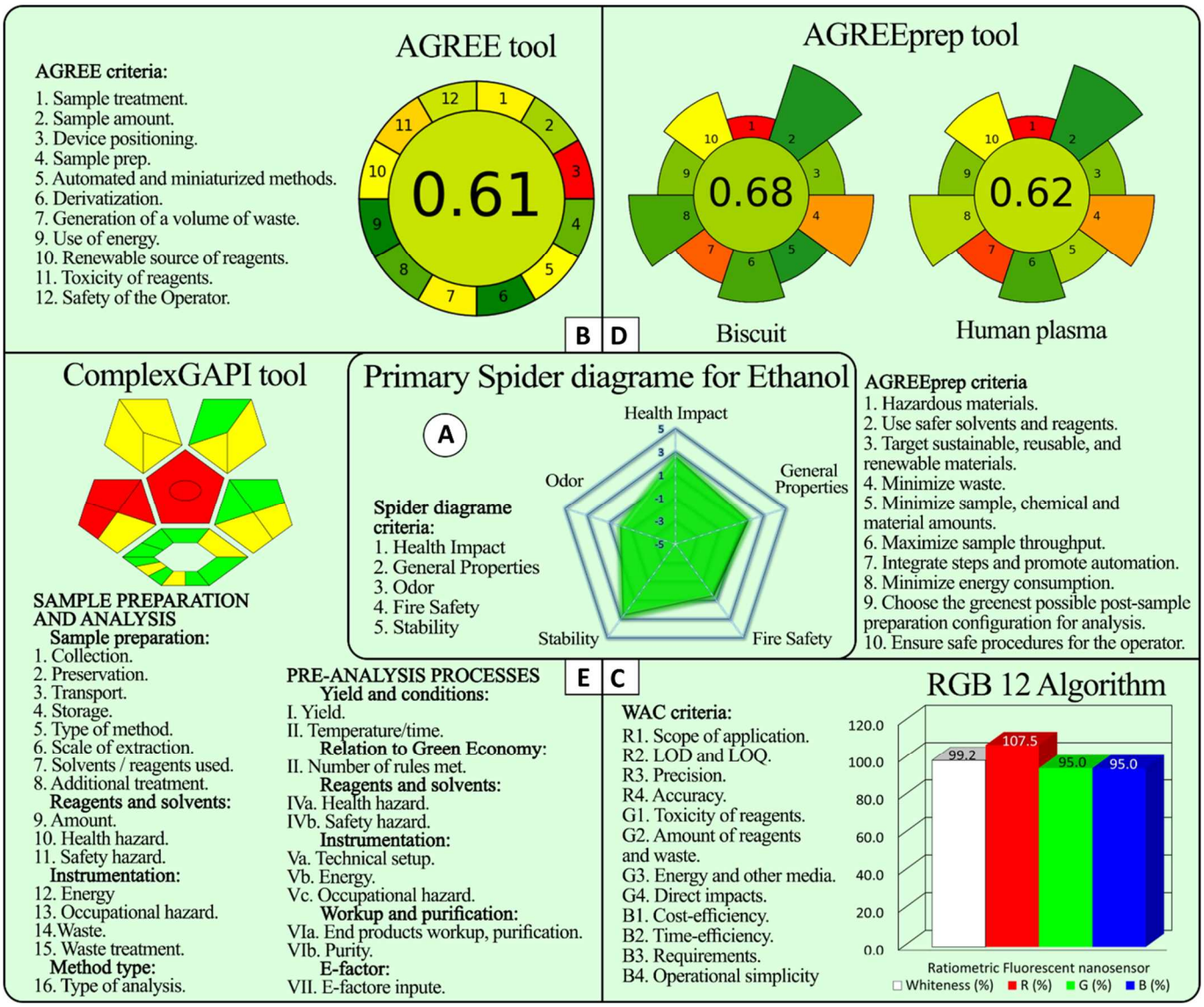

Figure S5. Greenness and whiteness evaluation results and criteria for the developed self-ratiometric fluorescent probe by greenness index via primary spider diagram (A), AGREE (B), RGB12 (C), AGREEprep (D), and ComplexGAPI tools (E).

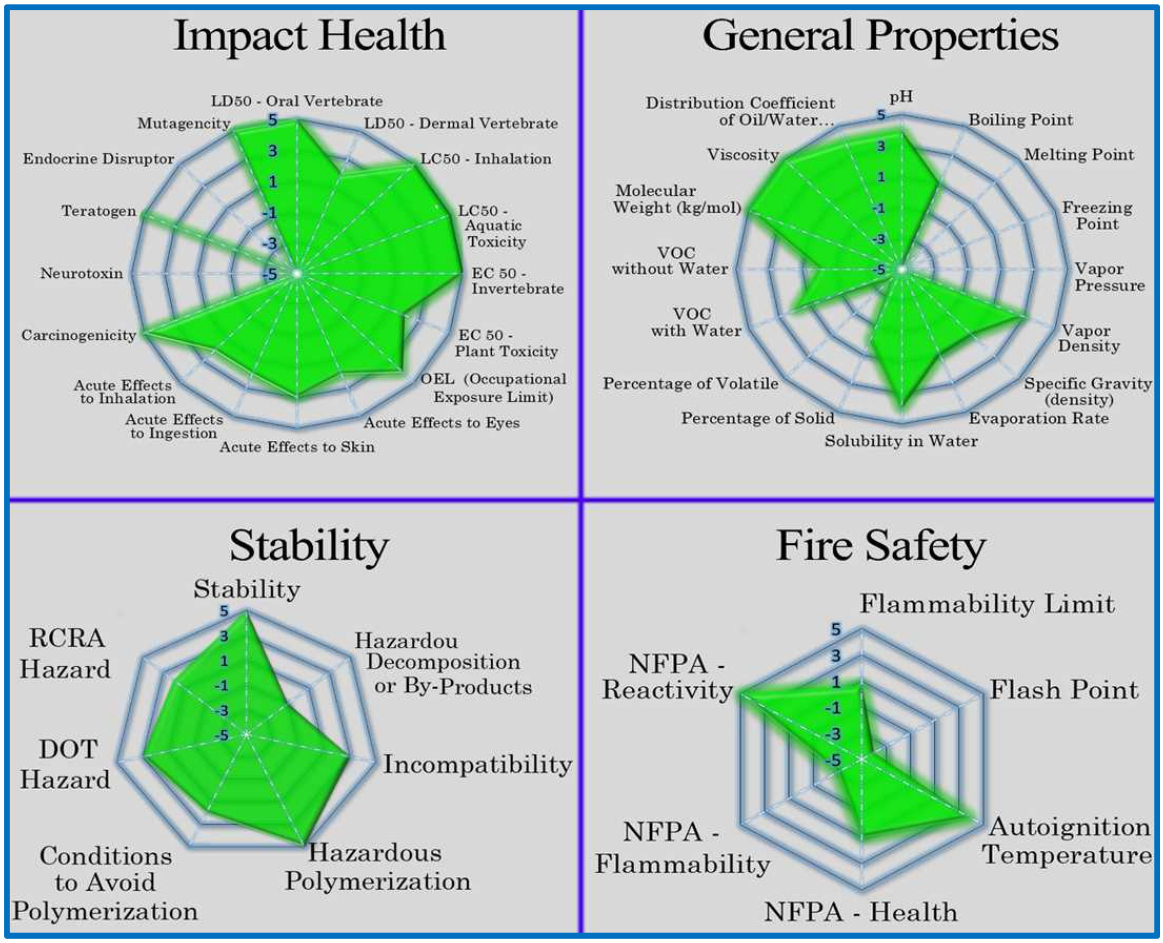

Figure S6. Greenness index results for ethanol via secondary spider diagrams.

Table S1: Application of the proposed method for measurement of vanillin in pure form

Parameter	Vanillin		
	Amount taken (µg/mL)	**Amount found (µg/mL)**	**% found***
	0.05	0.049	98.60
	0.2	0.204	101.90
	4.0	4.018	100.46
	6.0	5.949	99.16
	8.0	8.026	100.33
Mean			100.32
± SD			1.65
% RSD			1.65
% Error			0.74

*Average of three separate determinations (n = 3).

Table S2: Precision data for the proposed method for measurement of vanillin in pure form

	Intra-day			**Inter-day**		
Conc. (µg/mL)	**$\bar{x}$* ± S.D**	**% RSD**	**% Error**	**$\bar{x}$* ± S.D**	**% RSD**	**% Error**
0.2	101.90 ± 0.95	0.93	0.54	98.12 ± 1.31	1.34	**0.77**
4.0	100.46 ± 0.64	0.64	0.37	101.95 ± 0.93	0.91	**0.53**
6.0	99.16 ± 0.87	0.88	0.51	100.82 ± 1.08	1.07	**0.62**

*Average of three separate determinations (n = 3).

Table S3: Principles of WAC and their results according to RGB12 tool for ratiometric fluorescent nanosensor.

Method: Self-ratiometry					
R1: Scope of application	100.0	G1: Toxicity of reagents	90.0	B1: Cost-efficiency	100.0
R2: LOD and LOQ	120.0	G2: Number of reagents and waste	100.0	B2: Time-efficiency	120.0
R3: Precision	100.0	G3: Energy and other media	90.0	B3: Requirements	80.0
R4: Accuracy	110.0	G4: Direct impacts	100.0	B4: Operational simplicity	80.0
107.5		95.0		95.0	
99.2					

Supplementary References:

1. Rurack K Fluorescence Quantum Yields: Methods of Determination and Standards. In: Resch-Genger U (ed) Standardization and Quality Assurance in Fluorescence Measurements I. Springer, Berlin, Heidelberg, pp 101–145
2. Zu F, Yan F, Bai Z, et al (2017) The quenching of the fluorescence of carbon dots: A review on mechanisms and applications. Microchim Acta 184:1899–1914. https://doi.org/10.1007/s00604-017-2318-9
3. Gehlen MH (2020) The centenary of the Stern-Volmer equation of fluorescence quenching: From the single line plot to the SV quenching map. J Photochem Photobiol C Photochem Rev 42:100338. https://doi.org/10.1016/j.jphotochemrev.2019.100338
4. El-Shaheny R, Al-Khateeb LA, El Hamd MA, El-Maghrabey M (2021) Correction pen as a hydrophobic/lipophobic barrier plotter integrated with paper-based chips and a mini UV-torch to implement all-in-one device for determination of carbazochrome. Anal Chim Acta 1172:338684. https://doi.org/10.1016/j.aca.2021.338684
5. Magdy G, Abdel Hakiem AF, Belal F, Abdel-Megied AM (2021) Green one-pot synthesis of nitrogen and sulfur co-doped carbon quantum dots as new fluorescent nanosensors for determination of salinomycin and maduramicin in food samples. Food Chem 343:128539. https://doi.org/10.1016/j.foodchem.2020.128539